CENTENNIAL FEATURE ARTICLE

Model Potential Approaches for Describing the Interaction of Excess Electrons with Water Clusters: Incorporation of Long-Range Correlation Effects†

Thomas Sommerfeld,‡ Albert DeFusco,§ and Kenneth D. Jordan*,§

Department of Chemistry and Physics, Southeastern Louisiana University, Hammond, Louisiana 70402, and Department of Chemistry and Center for Molecular and Materials Simulations, University of Pittsburgh, Pittsburgh, Pennsylvania 15260

Received: July 9, 2008

In this work we focus on the binding of excess electrons to water clusters, a problem for which dispersion interactions, which originate from long-range correlation effects, are especially important. Two different model potential approaches, one using quantum Drude oscillators and the other using polarization potentials, are investigated for describing the long-range correlation effects between the weakly bound excess electron and the more tightly bound electrons of the monomers. We show that these two approaches are related in that the polarization potential models can be derived from the quantum Drude model approach by use of an adiabatic separation between the excess electron and the Drude oscillators. The model potential approaches are applied to clusters containing up to 45 water monomers. Where possible, comparison is made with the results of ab initio electronic structure calculations. Overall, the polarization potential approach is found to give electron binding energies in good agreement with those from the Drude model and ab initio calculations, with the greatest discrepancies being found for "cavity-bound" anion states.

I. Introduction

Reactions involving electrons in aqueous media are of fundamental importance in a wide range of biological and chemical processes.[1] For example, the passage of radiation through water ionizes the water, producing "free" electrons that can subsequently cause electronic excitation or bond cleavage of solute molecules. In addition, electrochemistry in aqueous media necessarily involves electron transfer through water, and electron transfer in photosynthetic reaction centers not only occurs in the presence of water but also explicitly involves water in the redox chemistry.[2]

Although solvated electrons in ammonia have been known since the studies of Weyl in 1864,[3] the hydrated electron (e_{aq}^-), was not identified until the experiments of Hart and Boag in 1962.[4] The hydrated electron has been the subject of numerous experimental and theoretical studies, with much of the emphasis having been placed on elucidating its dynamics following photoexcitation.[5−13] The ground electronic state of the hydrated electron is generally viewed as consisting of an electron in a approximately spherical cavity of radius ∼2.2 Å, with the electron binding energy (i.e., the energy required to promote the electron to the conduction band) being 3.3 eV.[5,14,15] However, the molecular level structure and the dynamics of the hydrated electron remain a subject of debate.[16] Indeed, it has even been suggested that the spectroscopic signature attributed to the hydrated electron is actually due to a solvated H_3O species.[17]

Recently, considerable attention has been focused on $(H_2O)_n^-$ clusters that can be studied by experimental techniques and high-level ab initio electronic structure methods that would not be applicable to e_{aq}^-.[18−31] The combination of theory and experiment on the small $(H_2O)_n^-$ clusters has greatly advanced our understanding of how an excess electron impacts and is accommodated by the *H*-bonding arrangements. Although the water monomer itself does not bind an excess electron to form a stable anion and does not have low-lying temporary anion states (resonances), the dimer and larger clusters do bind excess electrons.[23−35] The excess electron in the cluster anions occupies a nonvalence orbital, and the stability of the resulting ions derive from the interaction of the excess electron with the static charge distribution of the cluster as well as from induction and dispersion interactions between the excess electron and the electrons of the monomers. Although the basic structural motifs of the experimentally observed anions of the $n \leq 7$ clusters are now well established,[23−27] the structures of the larger clusters remain unknown. In particular, there has been an ongoing debate about the surface vs interior nature of the $n > 30$ clusters.[29−33]

Ab initio electronic structure methods have proven especially valuable in elucidating the role of electron correlation effects on the binding of excess electrons to water clusters.[20−23,36,37] Large basis set CCSD(T)[38] calculations of the electron binding energies (EBE) have been carried out for clusters as large as $(H_2O)_6^-$,[39] and Herbert and Head-Gordon have reported MP2 calculations on selected isomers of $(H_2O)_n^-$ clusters with *n* as large as 24,[20,21] with this work recently being extended to clusters as large as

† This year marks the Centennial of the American Chemical Society's Division of Physical Chemistry. To celebrate and to highlight the field of physical chemistry from both historical and future perspectives, *The Journal of Physical Chemistry* is publishing a special series of Centennial Feature Articles. These articles are invited contributions from current and former officers and members of the Physical Chemistry Division Executive Committee and from *J. Phys. Chem.* Senior Editors.

‡ Southeastern Louisiana University.

§ University of Pittsburgh.

10.1021/jp806077h CCC: $40.75
Published on Web 10/30/2008

Thomas Sommerfeld received his Diploma in Chemistry and his Doctorate in Theoretical Chemistry at the University of Heidelberg, Germany, in 1993 and 1997, respectively. He was a postdoctoral researcher at the University of Oxford, U.K. (1997−1998), studying predissociation lifetimes of small dianions, and at the University of Perugia, Italy (1998−1999), studying numerical methods for large complex-symmetric matrices. He then joined a research center at the Universities of Kaiserslautern and Heidelberg investigating the attachment of slow electrons to molecules. In 2005 he became research assistant professor at the University of Pittsburgh where his research focused on model building for water cluster anions. In 2006 he joined the faculty of Southeastern Louisiana University where he is currently assistant professor. His research interests are electron capture and electron-induced reactions.

Albert DeFusco received B.S. and Ph.D. degrees in Chemistry from Frostburg State University and the University of Pittsburgh, respectively, in 2003 and 2008. His Ph.D. research centered on development of a new classical force field for neutral water clusters and its application in the quantum Drude model for the interaction of an excess electron with water clusters. He is currently a postdoctoral researcher at Ames Laboratory at Iowa State University.

Kenneth D. Jordan received his B.A. in Chemistry from Northeastern University in 1970 and his Ph.D. in Physical Chemistry from MIT in 1974. He joined the Department of Engineering and Applied Science, Yale University, as a J. W. Gibbs Instructor, being promoted to Assistant Professor in 1976. In 1978, Professor Jordan moved to the Chemistry Department at the University of Pittsburgh, where he is now Distinguished Professor of Computational Chemistry and Director of the Center for Molecular and Materials Simulations. He is also a senior editor of *The Journal of Physical Chemistry* and is President-elect of the Telluride Research Science Center. Professor Jordan's research interests are presently focused on theoretical and computational approaches for characterizing hydrogen-bonded clusters, modeling chemical reactions on surfaces, and electron-induced chemistry. He is also working on the development of accurate force fields and on the characterization of gas hydrates.

$(H_2O)_{33}^-$ by Williams and Herbert.[22] However, comparison with experiment requires inclusion of finite temperature effects through Monte Carlo or molecular dynamics (MD) simulations, sampling 10^7 or more configurations, making ab initio (e.g., MP2 or CCSD(T)) methods computationally prohibitive even for clusters as small as the hexamer. Simulations of negatively charged water clusters containing a few tens of monomers are feasible with density functional methods, but the reliability of such simulations would be questionable because commonly used functionals do not properly describe long-range correlation effects,[40] which play a crucial role in the binding of excess electrons to water clusters,[36,37] and they also have a tendency to exaggerate charge delocalization.[41] In light of these considerations, it is not surprising that most of the theoretical work on moderate to large $(H_2O)_n^-$ clusters as well as on excess electrons in bulk water and in water films has employed model potentials.[10−13,42−47]

In the model potential approaches, the total energy of the anion is given by the energy of the neutral water system, as described by a classical force field, plus the binding energy of the excess electron, calculated using a one-electron model Hamiltonian. Although some of the early theoretical work using such model potentials did not allow explicitly for the polarization of the water molecules by the excess electron, it is now recognized that inclusion of electron−water polarization is important for reliable characterization of excess electrons in aqueous media.[45] In general, electronic polarization has been incorporated into the model Hamiltonians by means of damped or cutoff $-\alpha/2r_i^4$ terms, where α is the polarizability of a monomer and r_i is the distance from the electron and the polarizable site associated with monomer i. The successes of such models for describing the interaction of excess electrons with aggregates of water is surprising in light of the large body of theoretical work on small water clusters demonstrating that dispersion-type correlation interactions between the excess electrons and the electrons of the monomers make substantial contributions to the electron binding energies.[19−22,36,37,48−53] These findings suggest that model Hamiltonian approaches with polarization terms implicitly include long-range correlation effects.

In the present study we employ ab initio electronic structure methods and the quantum Drude model (QDM) developed in our group[48−53] to elucidate the role of correlation effects in the binding of excess electrons to water clusters. The Drude model incorporates the induction and dispersion interactions between the excess electron and the electrons of the monomers by use of quantum Drude oscillators.[54] In essence, this is a course-graining approach that models the dynamical response of the ten electrons of each monomer by two point charges, coupled harmonically. Unlike other model potential approaches, the quantum Drude model accounts explicitly for correlation effects, but at a fraction of the computational cost of ab initio methods. We show below that the quantum Drude model can be combined with an adiabatic approximation to derive one-electron polarization models, thereby providing insight into how such models incorporate correlation effects. The electron binding energies calculated using the resulting polarization models are compared with those from ab initio calculations and from the Drude model for clusters ranging from $(H_2O)_6^-$ to $(H_2O)_{45}^-$ in size. Both surface-bound and interior- (or cavity)-bound species are considered.

II. Theoretical Considerations

A. General Background. The role of electrostatics, in particular, long-range dipole potentials, in the binding of excess electrons to molecules and clusters, has been addressed in numerous theoretical studies.[36,37,49,55−61] Here, we note that, within the context of the Born−Oppenheimer approximation,[62] any molecule or cluster with a dipole moment greater than 1.625 D can bind an excess electron giving a so-called dipole-bound anion.[57−60] When corrections to the Born−Oppenheimer approximation are included, the critical dipole for binding the excess electron is found to depend on the moments of inertia but, as a rule-of-thumb, can be taken to be about 2.2 D.[61] The electrostatic potential associated with clusters of polar molecules with zero or near zero net dipole moments may also be able to bind an excess electron. The $(H_2O)_6$ species depicted in Figure 1, which represents such an arrangement, has been proposed as a model for the first shell of water molecules of e_{aq}^-.[14]

Although electrostatic interactions clearly play a crucial role in the binding of excess electrons to polar molecules and their clusters, they are far from the complete story. It has long been known that the excluded "volume" effect due to the valence electrons of the molecules causes a reduction of the EBEs compared to those expected on the basis of a purely electrostatic potential.[53] More recently, it was recognized that electron correlation effects, in particular, dispersion-type interactions between the weakly bound excess electron and the more tightly bound electrons of the polar molecules, also significantly impact the binding of the excess electron.[36,37] That such dispersion interactions could make a sizable contribution to the EBE follows from the large polarizability of the weakly bound electron. In classical force fields, dispersion interactions between atoms or molecules are generally handled by including R^{-6}, and, sometimes also, R^{-8} and R^{-10} terms, where R is an interatomic or intermolecular distance. However, due to the spatially extended nature of the weakly bound electron, this approach cannot be used to account for the dispersion contributions to the electron binding energies of $(H_2O)_n^-$ clusters. The Drude

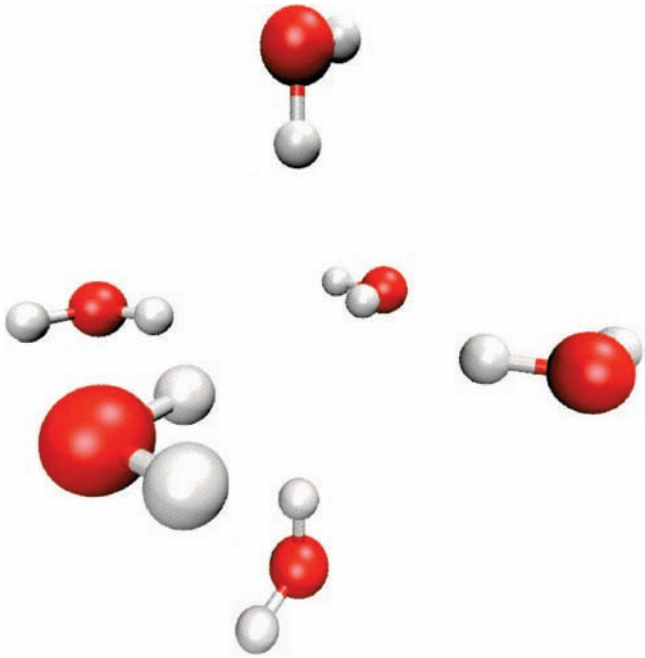

Figure 1. $(H_2O)_6$ cluster with the monomers arranged so as to give the Kevan model for the first hydration shell of e_{aq}^-.

model developed in our group[48−53,55] does account for the dispersion contributions to the EBEs, and, as will be shown below, so do models that allow for polarization of the water monomers by the excess electron. Ab initio MP2 and coupled-cluster calculations that incorporate long-range dispersion interactions are valuable for testing model potential approaches for describing $(H_2O)_n^-$ ions, and we find it useful to first briefly review ab initio approaches for calculating EBEs.

B. Ab Initio Treatment of $(H_2O)_n^-$ Clusters. Through second-order, the EBE, here taken as positive for a stable anion, may be written as

$$\mathrm{EBE} = \mathrm{EBE_{KT}} + \Delta E_{\mathrm{relax}} + \Delta E_2 \quad (1)$$

where $\mathrm{EBE_{KT}}$, $\Delta E_{\mathrm{relax}}$, and ΔE_2 represent the Koopmans' theorem (KT),[63] relaxation, and second-order correlation contributions to the electron binding energy, respectively. $\mathrm{EBE_{KT}}$ is given by the negative of $\varepsilon_{\mathrm{LUMO}}$, the energy of the lowest unoccupied molecular orbital of the neutral cluster; $\Delta E_{\mathrm{relax}}$ is defined as the difference between the ΔHF and KT binding energies; and ΔE_2 is given by the difference of the ΔHF and ΔMP2 binding energies, where

$$\Delta\mathrm{HF} = E_{\mathrm{HF}}(\mathrm{neutral}) - E_{\mathrm{HF}}(\mathrm{anion}) \quad (2)$$

and

$$\Delta\mathrm{MP2} = E_{\mathrm{MP2}}(\mathrm{neutral}) - E_{\mathrm{MP2}}(\mathrm{anion}) \quad (3)$$

where HF and MP2 denote Hartree−Fock and second-order Møller−Plesset perturbation theory, respectively.

For many molecules and their clusters, $\varepsilon_{\mathrm{LUMO}}$ is positive, implying that the excess electron is unbound at the KT level of theory. However, for water clusters with the monomers arranged so as to generate a sufficiently large region where the potential is sufficiently attractive, an excess electron binds even at the KT level, provided a suitably flexible basis set is employed. For small clusters the relaxation corrections are generally much less important than the correlation corrections to the EBEs.[48,49,53]

The second-order correlation correction to the EBE can be further decomposed into a contribution associated with the redistribution of the charge of the neutral molecule and a contribution due to dispersion interactions between the excess electron and the electrons of the monomers.[36] The former contribution, hereafter referred to as charge renormalization, acts so as to reduce the EBE, primarily as a result of the reduction of the dipole moment of the water monomer from 1.93 to 1.85 D in going from the Hartree−Fock to the MP2 approximation (with a sufficiently flexible basis set). The second-order dispersion corrections are necessarily positive (in the adopted sign convention). Ab initio calculations on small water clusters have shown that the dispersion contributions to the EBEs are generally much greater in magnitude than the charge renormalization contributions.[37] Hence, the net effect of the second-order corrections is to increase the EBEs.

In recent years, coupled-cluster methods have evolved into the method of choice for treating problems for which correlation corrections beyond second order are important. In particular, where such calculations are computationally tractable, the CCSD(T) method[38] has become the "gold standard" in electronic structure theory. The electron binding energy at the CCSD(T) level of theory is given by:

$$\Delta\mathrm{CCSD(T)} = E_{\mathrm{CCSD(T)}}(\mathrm{neutral}) - E_{\mathrm{CCSD(T)}}(\mathrm{anion}) \quad (4)$$

with the difference between the ΔMP2 and ΔCCSD(T) results providing an estimate of the contribution of correlation corrections beyond second order. The EOM-CCSD[64] method calculates the electron binding energy directly, rather than from an energy difference, and is applicable even in cases that the MP2 and CCSD(T) methods may not be reliable due to the failure of the HF approximation to provide a good zeroth-order description of the anion.

Excess electrons in $(H_2O)_n^-$ clusters occupy very extended orbitals, with relatively little charge density in the valence region of the water molecules. As a result, flexible basis sets containing several sets of diffuse functions are required to converge the EBEs of the excess electron states. The requirements for choosing such basis sets have been described previously and will not be repeated here.[65] The ab initio calculations carried out in the course of this study have used sufficiently flexible basis sets that the electron binding energies are close to converged with respect to the basis set. The Hartree−Fock, MP2, and CCSD(T) calculations were performed using the Gaussian 03 program.[66]

C. Quantum Drude Model. Over the past several years our group has developed a quantum Drude model for describing excess electrons interacting with clusters of water and of other polar molecules.[48−53] The quantum Drude model combines the DPP classical force field for the water−water interactions[67] with a model Hamiltonian, H_{D}, for the electron−water interaction. The classical force field defines the energy of the neutral cluster and also provides the electrostatic potential V_{es} for the excess electron. As illustrated in Figure 2, a Drude oscillator consists of two charges, a fixed $+q_{\mathrm{D}}$ charge and a mobile $-q_{\mathrm{D}}$ charge, coupled harmonically with a force constant k_{D}.[54] (Here we have assumed that the polarizability is isotropic, a reasonable approximation for water.) The polarizability of a Drude oscillator, α_{D} is given by $q_{\mathrm{D}}^2/k_{\mathrm{D}}$, chosen to equal the experimental value of the isotropic polarizability of the water monomer, i.e., 9.745 au^3.[68] The fixed $+q_{\mathrm{D}}$ charge of a Drude oscillator is located at the *M* site of the DPP model which is displaced 0.25 Å from the O atom, as shown in Figure 2.

In principle, the Drude oscillators can be used to describe the dispersion and induction interactions between the monomers as well as between the excess electron and the monomers,

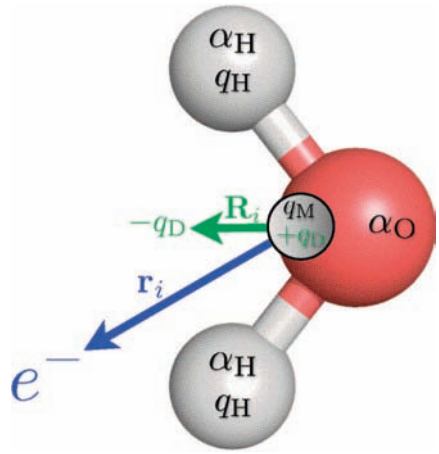

Figure 2. Pictorial representation of the DPP and Drude models.

allowing for a fully self-consistent treatment of electron−water and water−water dispersion and induction. However, we have found that it is adequate to adopt a computationally faster approach in which the water−water induction and dispersion interactions are described by the water force field, with the Drude oscillators (one on each monomer) being employed to describe only the dynamical response of the electron distribution of the water molecules to the excess electron.

In the DPP water model the static charge distribution of each monomer is represented by three point charges and induction is treated via three mutually interacting point polarizable sites. Intermonomer dispersion and short-range exchange-repulsion interactions between the monomers are described by means of damped C_6R^{-6} and exponential terms, respectively. The locations of the charges and the polarizable sites for the DPP model are indicated in Figure 2.

The Drude model Hamiltonian, H_D, includes the electronic Hamiltonian, H_e, the Hamiltonian for the collection of Drude oscillators, H_{osc}, and a term describing the coupling between the electron and the oscillators:

$$H_D = H_e(\mathbf{r}) + \sum_{i=1}^{N} h_{osc}(\mathbf{R}_i) + \sum_{i=1}^{N} V_{e,osc}(\mathbf{r}_i,\mathbf{R}_i) \quad (5)$$

where

$$H_e = -\frac{\hbar^2}{2m_e}\nabla_e^2 + V_{es} + V_{rep} \quad (6)$$

$$h_{osc} = -\frac{\hbar^2}{2m_D}\nabla_{osc}^2 + \frac{1}{2}k_D(X^2 + Y^2 + Z^2) \quad (7)$$

and

$$V_{e,osc} = q_D\frac{\mathbf{r}\cdot\mathbf{R}}{r^3}f(r) \quad (8)$$

The potential energy portion of H_e includes V_{es}, which describes the interaction of the excess electron with the point charges, used to model the fixed charge distributions of the monomers, as well as with the induced dipoles from intramonomer induction, and V_{rep}, which describes the short-range repulsion and exchange interactions between the excess electron and the valence electron distributions of the monomers. In this work, the repulsive potential of ref 48 is employed rather than the simpler, more approximate, repulsive potential of ref 49. In eqs 5−8, **r** is the collection of coordinates describing the interaction of the excess electron with the permanent point charges, the induced point dipoles, and the repulsive sites in the pseudopotentials, $\mathbf{r}_i$ is the vector from the electron to oscillator i, $\mathbf{R}_i = (X_i, Y_i, Z_i)$ is the displacement vector of Drude oscillator i, and $f(\mathbf{r})$ is a function that damps out the unphysical short-range behavior of the coupling term and is taken to be $[1 - \exp(-br^2)]$. It should be noted that eq 8 retains only the leading term resulting from the separation of the pair of charges associated with a Drude oscillators.

In solving for the energy levels of H_D, we make use of a product basis set, consisting of s and p Gaussian-type (GTO) functions for the excess electron and a "minimal" $|000\rangle$, $|100\rangle$, $|010\rangle$, $|001\rangle$ basis set for each oscillator. $|000\rangle$ denotes the ground state of the oscillator, and $|100\rangle$, $|010\rangle$, and $|001\rangle$ denote excited states with one quanta in the x, y, z degrees of freedom, respectively. The basis set for the excess electron has been described in ref 50 and consists of a single s-type GTO centered on each H atom, a 1s1p set of GTOs centered on the midpoint between the two H atoms of each monomer, and a 5s4p set of GTOs located at the center of mass of the cluster. These electron and oscillator basis sets are adequate for describing both surface-bound and interior-bound states of the excess electron for the clusters considered here (although, to obtain fully converged results, still larger electronic basis sets would be required for some of the clusters).

In our applications of the quantum Drude model to $(H_2O)_n^-$ clusters, the principal approach for evaluating the energy associated with H_D is the single-plus-double-excitation configuration interaction (CI) approximation, where the double excitations are restricted to configurations that involve simultaneous excitation of the excess electron and of one of the Drude oscillators. We also report for the model potential approaches EBEs from a KT-like approximation, which neglects the coupling of the excess electron to the Drude oscillators, as well as from a second-order perturbation theory treatment. These are included primarily for illustrating the different rates of convergence of the EBEs with the order of the interaction in the Drude model and ab initio approaches.

The Drude Hamiltonian contains two free parameters, α and b, both of which are determined by fitting to ab initio results for the water dimer. The α parameter scales the repulsive potential and is chosen so that for the water dimer the EBE from the model potential calculation without the Drude oscillators matches the KT EBE from a large basis set ab initio Hartree−Fock calculation on the neutral molecule, giving α = 0.158. The b parameter, which controls the damping of the electron−Drude coupling, is adjusted so that the electron binding energy of the water dimer, calculated using the Drude model in conjunction with the CI method, matches that (41 meV) from large basis set ab initio CCSD(T) calculations. This gives a value of $b = 0.9312$ Bohr^{-2}.

D. Adiabatic Approximation. Up to this point the choices of q_D and m_D have not been specified. In our applications of the Drude model to water clusters we have chosen $q_D = |e^-|$ and $m_D = m_e$. With this choice, the excitation energy of the Drude oscillator is 8.7 eV, a reasonable value for an effective valence excitation energy of the water monomer. For the clusters considered here, with the exception of $(H_2O)_{45}^-$, the excess electron binds by at most 1.1 eV, almost an order of magnitude smaller than the excitation energy of a Drude oscillator, suggesting the possibility of an adiabatic separation between the excess electron and the Drude oscillators. To illustrate how this separation is accomplished, we consider the case of an excess electron interacting with a single Drude oscillator. The extension to multiple oscillators is straightforward.

In the adiabatic approximation, the Hamiltonian for the fast degrees of freedom (here associated with the Drude oscillator),

$$H_f(\mathbf{R};\mathbf{r}) = h_{osc}(\mathbf{R}) + V_{e,osc}(\mathbf{R};\mathbf{r}) \quad (9)$$

depends only parametrically on the position $\mathbf{r}$ of the clamped excess electron. The eigenvalues U_j of H_f, when combined with the electrostatic and electron−molecule repulsive terms, give potential energy surfaces for the motion of the excess electron. Provided that the nonadiabatic couplings between the ground and excited potential energy surfaces are small, a Born−Oppenheimer-like treatment of the excess electron on the ground-state adiabatic surface, U_0, should closely reproduce the electron binding energies from the "full" Drude model.

To determine the potential $U_0(r)$, the matrix elements of H_f are evaluated in terms of the eigenfunctions $|n\rangle$ of h_{osc}

$$h_{osc}(\mathbf{R})|n\rangle = E_n|n\rangle \quad (10)$$

where $n = (n_x, n_y, n_z)$ is a collective index of the quantum numbers of the three-dimensional harmonic oscillator, and $E_n = (2n_x + 2n_y + 2n_z + 3)\varepsilon_D$, with $\varepsilon_D = {}^1/_2\hbar\omega_D$. In this basis set the matrix elements of H_f are

$$\langle n|H_f|m\rangle = E_n\delta_{n,m} + \frac{q_D}{r^3}f(r)\sum_{n,m}(x\langle n|X|m\rangle + y\langle n|Y|m\rangle + z\langle n|Z|m\rangle) \quad (11)$$

with the matrix elements contributing to the first term in parenthesis being given by

$$\langle n|X|m\rangle = \langle n_x n_y n_z|X|m_x m_y m_z\rangle = \begin{cases} \sqrt{\dfrac{n_x+1}{2\omega_D m_D}} & n_x = m_x - 1,\ n_y = m_y,\ n_z = m_z \\ \sqrt{\dfrac{n_x}{2\omega_D m_D}} & n_x = m_x + 1,\ n_y = m_y,\ n_z = m_z \\ 0 & \text{otherwise} \end{cases} \quad (12)$$

with analogous expressions for the matrix elements of Y and Z.

With the "minimal" basis set described above for the Drude oscillators, the matrix representation of H_f is

$$H_f = \begin{pmatrix} 3\varepsilon_D & xv(r) & yv(r) & zv(r) \\ xv(r) & 5\varepsilon_D & 0 & 0 \\ yv(r) & 0 & 5\varepsilon_D & 0 \\ zv(r) & 0 & 0 & 5\varepsilon_D \end{pmatrix} \quad (13)$$

where

$$v(r) = \frac{q_D}{r^3}f(r)\sqrt{\frac{\hbar}{2\omega_D m_D}} \quad (14)$$

The lowest eigenvalue of H_f is

$$U_0(r) = 4\varepsilon_D - \sqrt{{\varepsilon_D}^2 + \frac{\hbar {q_D}^2}{2\omega_D m_D r^4}f^2(r)} \quad (15)$$

After subtracting the zero-point energy E_0 and substituting $\alpha_D = q_D{}^2/\omega_D{}^2 m_D$, this gives the adiabatic potential

$$V_{ad}(\mathbf{r}) = \varepsilon_D - \sqrt{{\varepsilon_D}^2 + \frac{\varepsilon_D \alpha_D}{r^4}f^2(r)} \quad (16)$$

For large r, a Taylor series expansion gives

$$V_{ad}(r) = -\frac{\alpha_D}{2r^4}f^2(r) + \frac{{\alpha_D}^2}{8\varepsilon_D r^8}f^4(r) - \ldots \quad (17)$$

the leading term of which is the asymptotic form of the polarization potential multiplied by the square of the damping function. Similar to the Born−Oppenheimer separation where the electrons instantaneously follow the nuclei, the polarization potential given in eq 16 can be understood as a Drude oscillator (which models the response of the tightly bound electrons) instantaneously following the motions of the excess electron. That is, the correlated motion of two objects is modeled as a fast object (the Drude oscillator) perfectly tracking the slow object (the excess electron). Moreover, this analysis demonstrates that the $-\alpha/2r^4$ polarization potential commonly employed in modeling excess electrons interacting with molecules and clusters does include long-range (i.e., dispersion-like) correlation effects. This has been demonstrated previously in other contexts and using different derivations. For example, it has been shown that the asymptotic form of the potential describing the interaction of the outer electron and the cation core of spherical atoms such as Na contains a $-0.5\alpha_I/r^4$ term, where α_I is the polarizability of the ion core.[69] In fact, this is exploited in the polarizable core pseudopotentials of Stoll and co-workers.[70] Similarly, the asymptotic form of the correlation potential for electron−atom and electron−molecule scattering contains an analogous term where the polarizability is that of the neutral target.[71]

Although the use of polarization potentials to describe correlation effects is well documented in the literature, it is not fully appreciated in the quantum chemistry community. The key to understanding the recovery of electron correlation effects through the use of a polarization potential is to recognize that there is a fundamental difference between the interaction of a point charge and the interaction of an excess electron with a polarizable atom or molecule. In both cases the response of the atom or molecule to the point charge can be described by allowing for single excitations electron of the atom or molecule (or, in the Drude model approach, single excitations of the Drude oscillator). The single excitations of the "target" give rise to the polarization potential. In the case of a true point charge this potential directly gives the polarization energy, whereas for the excess electron the polarization potential is incorporated in the Schrödinger equation, the solution of which gives the electron binding energy and the charge distribution of the excess electron. Solution of the resulting Schrödinger equation thus accounts for the long-range correlation between the excess electron and the electrons associated with the water molecules. The differences between the ab initio, Drude model, and polarization model approaches are illustrated in Figure 3. Even though the above derivation and discussion make it clear that polarization potential models do include long-range correlation effects, it remains to be established whether polarization potential models accurately predict the EBEs for both surface and interior and surfaces states and for both small and large clusters.

In this work, we consider four adiabatic potential models: (1) the full adiabatic potential given by eq 16, with f chosen to be $(1 - e^{-br^2})$, (2) the leading term in the Taylor series expansion in eq 17, with f again chosen to be $(1 - e^{-br^2})$, (3) the full adiabatic potential given by eq 16, but with f chosen to be $(1 - e^{-br^3})$, and (4) $\alpha_D/(r^2 + r_c^2)^2$, where r_c is a cutoff parameter. These adiabatic potentials are combined with the electrostatic and repulsive terms of eq 6 to give four one-electron model Hamiltonians designated PM1, PM2, PM3, and PM4, respectively, where "PM" signifies that a polarization potential is used

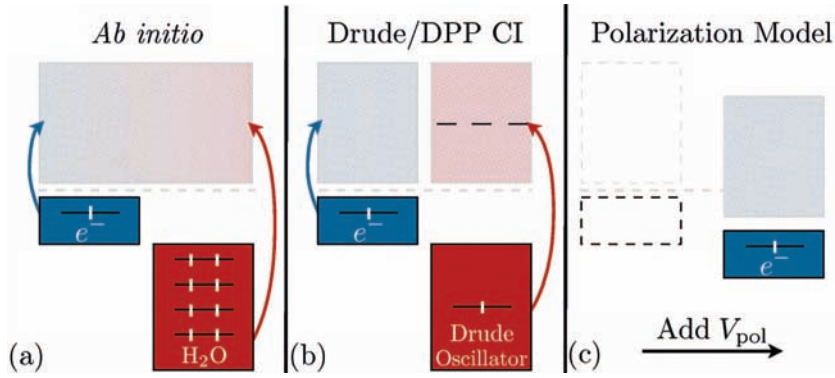

Figure 3. Illustration of the course graining in the Drude and polarization potential approaches to $(H_2O)_n^-$ clusters. (a) Ab initio: dispersion is described by a simultaneous excitation of the excess electron and of the electrons of a water monomer. (b) Drude model: the dynamical response of the electrons of the water monomers are modeled by excitations of a quantum Drude oscillator associated with each monomer. (c) Polarization model: dispersion interactions are incorporated via polarization potential associated with each monomer.

to model the dynamical response of the water molecules to the excess electron.

For each water cluster considered, the electron binding energies were calculated for each of these models using the same Gaussian basis set for the excess electron as used in the Drude model calculations as well as using a discrete variable representation (DVR) with sine-type particle-in-the-box functions.[72] Provided a sufficiently large and dense set of grid points are used, the DVR calculations give electron binding energies close to those obtained using the GTO basis set, and, for that reason, only the latter results are reported here.

An issue that arises in the use of the polarization potential models concerns the choice of the damping or cutoff parameters. One might anticipate that the b parameter used in the Drude model could simply be carried over to the PM1 and PM2 models. However, with this choice, the latter models significantly overbind the excess electron for all clusters considered. This may be a consequence of the integrands in the integrals encountered in the polarization potential models more heavily weighing small r values than those in the Drude model. To solve the overbinding problem, the damping (or cutoff) parameters in the various polarization potential models have been adjusted so that the electron binding energies for the water dimer calculated using these models reproduce the 41 meV value from large basis set ab initio CCSD(T) calculations. This approach gives $b = 0.214$ and 0.180 Bohr^{-2} for the PM1 and PM2 models, respectively, $b = 0.091$ Bohr^{-3} for the PM3 model, and $r_c = 1.684$ Bohr for the PM4 model. The former two values differ by about a factor of 4.5 from the corresponding values for the Drude model.

Figure 4a plots along the HOH bisector the polarization potentials of the PM1, PM2, PM3, and PM4 models together with the MP2 level ab initio polarization potential. The latter was obtained by performing MP2/aug-cc-pVTZ calculations on H_2O in the presence of negative $(-e)$ point charge, and subtracting from the resulting energies the purely electrostatic (i.e., neglecting induction) contributions. Panels b and c of Figure 4 display the PM3, Turi−Borgis (TB),[10] and MP2 polarization potentials both along the HOH bisector (Figure 4a) and along an OH bond (Figure 4b) of a water monomer.

There are several conclusions that can be gleaned from examination of the curves shown in Figure 4. For $r \gtrsim 1.5$ Å (measured from the O atom), the polarization potentials associated with the various PMx models are in fairly good agreement with each other and with the MP2 polarization potential, although it is clear that there is appreciable anisotropy in the

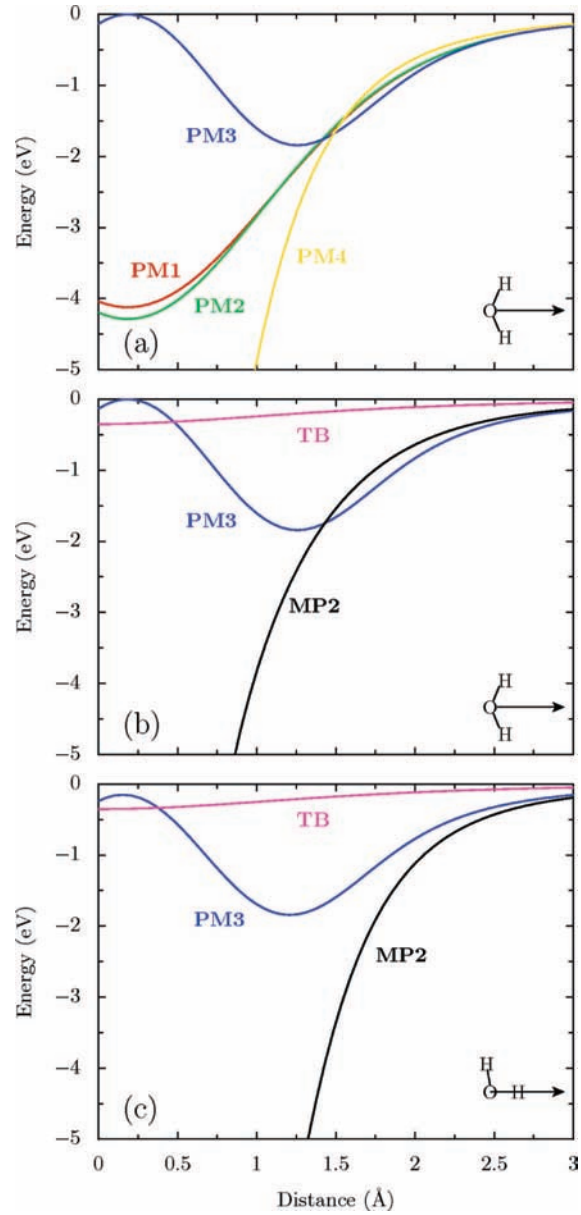

Figure 4. Polarization potentials for the water monomer used in the PMx and TB models and from MP2/aug-cc-pVTZ calculations: (a) PM1, PM2, PM3, and PM4 polarization potentials along the HOH bisector; (b) comparison of the PM3, TB, and MP2 polarization potentials along the HOH bisector; (c) comparison of the PM3, TB, and MP2 polarization potentials along an OH bond.

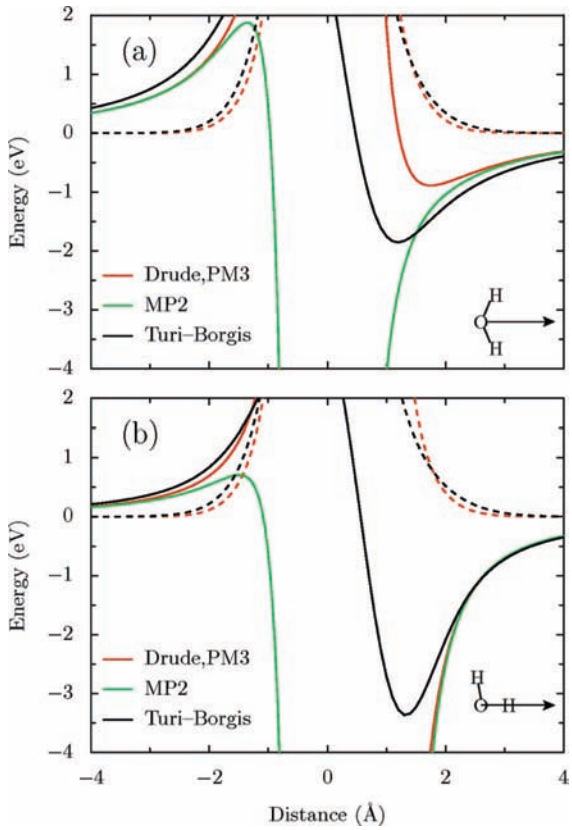

Figure 5. Electrostatic potentials for the water monomer as described by the DPP and SPC water models employed in the PM3 and TB electron−water models, respectively, and from MP2 calculations. The figure also includes the repulsive electron−water potentials used in the PM3 and TB models (dashed lines). Results are shown along the HOH bisector (a) and along an OH bond (b).

ab initio polarization potential which, of course, is not recovered with the model potentials as they employ only a single, isotropic polarizable site. For $r \lesssim 1.5$ Å, the various polarization potentials differ significantly from one another and are significantly less attractive than the MP2 polarization potential. However, at these short distances, the repulsive term makes a sizable contribution to the net potential, weakening the sensitivity of the EBE to the precise form of the damping of the polarization potential. In addition, the exact potential for the interaction of an excess electron with a water monomer would include exchange-induction and charge-penetration effects which are expected to be important at these small r values. Although the model potentials do not include explicit terms for describing these short-range effects, they are incorporated in an effective manner through the adjustment of the damping (or cutoff) parameter to reproduce the ab initio CCSD(T) value of the EBE of the water dimer.

The Turi−Borgis[10] electron−water potential has been used in several recent simulations of $(H_2O)_n^-$ clusters as well as of excess electrons in bulk water, making the comparison of this model with the Drude and PM3 models described above particularly relevant.[32,33] From Figure 4 it is seen that the polarization potential in the TB model is much weaker than the ab initio and PMx polarization potentials. Figure 5 displays the repulsive and electrostatic potentials employed in the PMx and TB model potentials together with the MP2-level electrostatic potential. From this figure it is seen that although the repulsive potentials in the two models are similar, the electrostatic potentials differ appreciably, with that associated with the Turi-Borgis model being more attractive for approach of the negative test charge along the HOH bisector from the H-end of the molecule. This is a consequence of the TB model being based on the SPC force field,[73] which employs enhanced charges and gives for the water monomer a dipole moment of 2.3 D, about 25% larger than the experimental gas-phase value. Interestingly, the cutoff parameter in the TB polarization potential was chosen so that the calculated ground-state energy of an excess electron in bulk water closely reproduced the corresponding experimental quantity for e_{aq}^-. Because of the enhanced charges (and, thus, enhanced electrostatics) in the SPC model, this fitting procedure is responsible for the underestimation of electron−water polarization in the TB model. It remains to be seen whether the compensation between the enhanced electrostatics and the too weak polarization in the TB model is nearly as complete for $(H_2O)_n^-$ clusters as for e_{aq}^-.

For $r \lesssim 2$ Å, the electrostatic potentials associated with the TB and PM3 models differ appreciably from that obtained from MP2 calculations. This reflects a limitation of a simple point-charge models, neglecting charge penetration, for representing the electrostatics. Again, this is expected to be relatively unimportant for the EBE because very little of the excess electron density resides this close to the monomers.

III. Results

As alluded to in the previous section, there are subtle differences between individual contributions to the EBEs obtained from the model potential and ab initio approaches. In addition, for some of the clusters considered there are problems caused by inappropriate zeroth-order wave functions. We find it useful, therefore, to start this section with a brief consideration of these issues. We then turn to the results for several isomers of $(H_2O)_6^-$, which is the largest water cluster for which there are electron binding energies from large-basis set CCSD(T) calculations,[38] several isomers of $(H_2O)_{20}^-$ and $(H_2O)_{24}^-$ that were studied previously by Herbert and Head-Gordon,[20,21] and two isomers of $(H_2O)_{45}^-$ that were studied by Turi and Rossky.[33] This is followed by a brief examination of the low-lying excited states predicted by the model potential approaches. The Results section is concluded with an analysis of the isomer populations of $(H_2O)_7^-$ obtained from Drude model Monte Carlo simulations.[74]

A. General Considerations. Overall, the four PMx models give similar values of the EBEs, with the agreement with the Drude model results being slightly better for the PM3 model, and for this reason, only the PM3 results will be considered in the ensuing discussion. Figure 6 compares for the $n = 2-24$ clusters the EBEs calculated using the Drude and PM3 models with those from ab initio calculations. Overall, the EBEs from the two model potential approaches are in good agreement with the ab initio results, with the largest discrepancies being for some of the clusters with zero or near zero dipole moments. As will be discussed below, the discrepancies in those cases are likely due to limitations in the ab initio calculations.

Table 1 summarizes the calculated EBEs of the ground-state anions of the test systems. Results are reported for the Drude, PM3, and TB models. For the $n \leq 24$ clusters, results from ab initio calculations are also reported. In the case of the Drude model, the EBEs are reported for the electrostatic plus repulsion (ES+rep), second-order perturbation theory, and single-plus-double excitation CI levels of theory. The second-order corrections are further separated into induction and dispersion contributions. The ES+rep method is a KT-like approximation as it neglects the Drude oscillators in the Hamiltonian given in eq 5. It is important to note, however, that the atomic charges

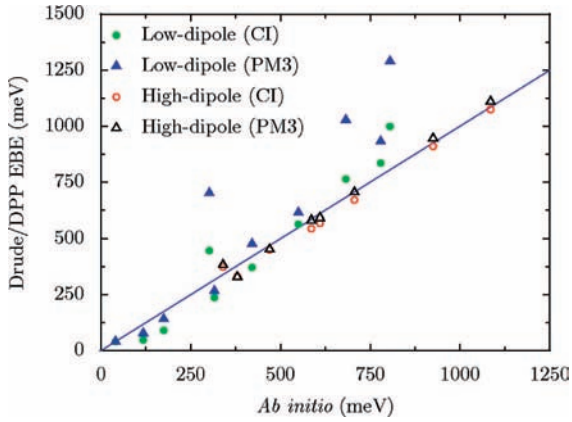

Figure 6. Electron-binding energies of the $(H_2O)_n^-$, $n = 2$–24 clusters calculated using Drude CI (circles), PM3 (triangles), and ab initio methods. Results for clusters with $\mu < 4$ D are indicated by solid symbols and those for clusters with $\mu \geq 4$ D by open symbols. For the $n = 2$ and 6 clusters, the ab initio results are from large basis sets CCSD(T) calculations; for the $n = 20$ clusters with large dipole moments, the ab initio EBEs are from the MP2 calculations of ref 21; for the $n = 20$ and 24 clusters with zero or near zero dipole moments, the ab initio EBEs are from the s-MP2 (BHLYP) calculations of ref 21. The $n = 6$, 20, and 24 clusters considered are depicted in Figures 7, 10, and 11, respectively.

employed in the model Hamiltonian have been chosen so as to reproduce the experimental dipole moment of the gas-phase monomer, whereas ab initio Hartree−Fock calculations give a dipole moment for the monomer that is about 15% too large. In ab initio approaches, such as MP2 or CCSD(T), the correlation contributions to the EBE include terms that correct for the deficiencies of the Hartree−Fock charge distribution. In contrast, the effect of charge-renormalization on the EBEs is incorporated in the zeroth-order energy in the Drude model. As a result, the EBEs from the ES+rep and second-order Drude model calculations are not directly comparable to the EBEs from ab initio KT or MP2 calculations. The Drude model CI and ab initio CCSD(T) EBEs, however, are directly comparable. As will be discussed below, for the six $(H_2O)_n^-$ isomers, the changes in the EBEs in going from MP2 to CCSD(T) calculations are relatively small, making comparison with the results of ab initio MP2 calculations a viable alternative for testing the model potentials for larger clusters for which ab initio CCSD(T) calculations are not feasible.

Examination of Table 1 reveals that for most of the clusters with zero or near zero dipole moments, both the Hartree−Fock and ES+rep approaches fail to bind or only weakly bind the excess electron, with the failure to bind the excess electron being more prevalent with the ES+rep method due to the weaker electrostatics in this approach. For these clusters, perturbative approaches based on the Hartree−Fock or ES+rep wave functions prove to be inadequate. The Drude model CI and the polarization model approaches do not suffer from this problem because they do not depend on the validity of a zeroth-order wave function. Indeed, both Drude model CI and polarization model calculations predict the excess electron to bind to all clusters considered. An interesting question is whether the CCSD(T) method, which is built on the Hartree−Fock wave function but includes certain correlation corrections to all orders, can provide an accurate description of the anion in cases where the Hartree−Fock approximation does not bind (or only weakly binds) the excess electron. Our studies of model systems show that the CCSD(T) method can properly describe the anion for some, but not all, such cases.[75]

For clusters with sizable dipole moments, the excess electron acquires a significant binding energy in both the ES+rep and Hartree−Fock approaches. However, even for these species, electron correlation effects play an important role, typically leading to increases in the EBEs by a factor of 2−3 in the Drude model and by 23−47% in the ab initio calculations. Correlation corrections beyond second order are very important in the Drude model, in some clusters being comparable to the second-order corrections, whereas they are much smaller (5−22%) in the ab initio calculations. The different behavior of the correlation corrections in the Drude model and ab initio approaches is due to the partial cancelation between charge renormalization and other contributions to the correlation energy in the latter. As a result, ab initio MP2 calculations are useful for assessing the reliability of model potential approaches for calculating EBEs, at least in those cases where there is appreciable electron binding in the KT approximation. (This has been noted previously by Herbert and Head-Gordon.[20,21]) This is an important observation because the MP2 method can be applied to much larger clusters than can the CCSD(T) method.

B. Results for $(H_2O)_6^-$. The six $(H_2O)_6^-$ isomers considered are shown in Figure 7. Of these, four (6A−6D) have large dipole moments and surface-bound excess electron states, and two (6E and 6F) have no net dipole moment. 6E consists of two trimers with the three free OH groups of each trimer being pointed toward the other trimer generating a region with a strongly attractive electrostatic potential between the trimers. 6F is the model for the first solvation shell of e_{aq}^- mentioned in the Introduction and depicted in Figure 1. 6A−6E are true minima on the $(H_2O)_6^-$ potential energy surface, whereas 6F is not a local minima. In 6F, the O atoms of water molecules are in an octahedral arrangement, with one H atom of each monomer pointed toward the center of the cavity. The distance between the H atoms pointing inward and associated with adjacent O atoms is taken to be 4.2 Å, close to the diameter of the cavity associated with e_{aq}^-. Figure 7 also displays for the $(H_2O)_6^-$ species the charge distributions of the excess electron as described by the Drude model CI calculations. In this figure isosurfaces enclosing 70 and 90% of the electron density are shown. For all six $(H_2O)_6^-$ species the Drude model CI and PM3 polarization models give EBEs close to the CCSD(T) values, with the average absolute difference of the model potential EBEs from the corresponding CCSD(T) values being only about 5%. (The ab initio results for 6A−6E are from ref 38, and those for 6F are from our calculations.) The largest differences (∼14%) are for the chain isomer 6D, for which the Drude CI and PM3 approaches underestimate the EBE. The larger errors in the EBEs calculated using the model potential approaches for 6D are due mainly to our locating the off-atom 5s4p set of functions at the center of mass of the cluster which is far from the excess electron, rather than to an inherent deficiency in the model potentials.

The changes in the EBEs in going from the KT to the Hartree−Fock approximation are relatively small for 6A−6D, which have large dipole moments, but are sizable for 6E and 6F (39 and 152%, respectively), which have no net dipole moment and for which the excess electron is nominally cavity bound. (Obviously, for such small clusters, much of the excess electron distribution is located outside the cavity, as can be seen from Figure 6.) The inclusion of electron correlation effects using ab initio methods leads to 53−71% increases in the electron binding energies for 6A−6D and to slightly greater than 100% increases for 6E and 6F, with most of the correlation contribution being recovered at the MP2 level of theory. As

TABLE 1: Dipole Moments (D) and Electron Binding Energy (meV) Contributions for Various $(H_2O)_n^-$ Clusters

	Drude							TB			ab initio			
molecule	μ(D)	Es+rep	ind	disp	second order	CI	PM3	Es+rep	pol	total	KT	HF	MP2	CCSD(T)/(s-MP2[a])
2	4.0	6	0	9	15	41	41	30	9	39	6	11	23	41
6A	9.4	171	25	135	331	451	453	272	68	340	286	290	404	470
6B	8.5	180	37	189	406	569	592	407	117	524	312	368	543	610
6C	9.2	123	17	102	242	374	384	221	64	285	185	199	279	340
6D	12.2	129	10	104	243	332	330	158	41	198	230	247	333	380
6E	0	60	48	276	384	565	614	478	166	644	194	269	494	550
6F	0	−4	0	8	4	835	932	175	239	414	46	262	752	780
20A	24.9	566	81	244	891	1074	1110	656	137	793		883	1083	(1085)
20B	18.8	432	77	221	730	910	946	531	131	662		723	908	(925)
20C	14.5	252	58	180	490	670	705	324	114	438		497	657	(706)
20D	14.2	183	40	145	368	545	581	246	99	345		379	516	(586)
20E	2.0	−4	0	1	−3	48	78	0	16	16		−51	−22	(118)
20F	0.1	7	1	82	89	372	417	0	159	159		93	227	(421)
24A	0	−5	0	1	−4	764	1028	−17	285	268		80	576	(632)
24B	0	−5	0	1	−4	91	142	5	26	31		−35	3	(175)
24C	0	−5	0	1	−4	447	701	−8	29	21		−35	4	(302)
24D	0	−5	0	2	−3	999	1290	11	464	475		254	793	(805)
24E	0	−3	0	13	10	237	267	97	46	143		49	136	(316)
45A	9.2	697	1159	900	2766	2508	2861	1640	716	2356				
45B	22.0	742	158	313	1213	1350	1480	775	211	986				

[a] CCSD(T) results for the $(H_2O)_6^-$ isomers and s-MP2(BHLYP) results for the $(H_2O)_{20}^-$ and $(H_2O)_{24}^-$ isomers. The ab initio results from 6A-6E are from ref 39, and those for the $(H_2O)_{20}^-$ and $(H_2O)_{24}^-$ clusters are from ref 21. The s-MP2(BHLYP) results are reported in parentheses.

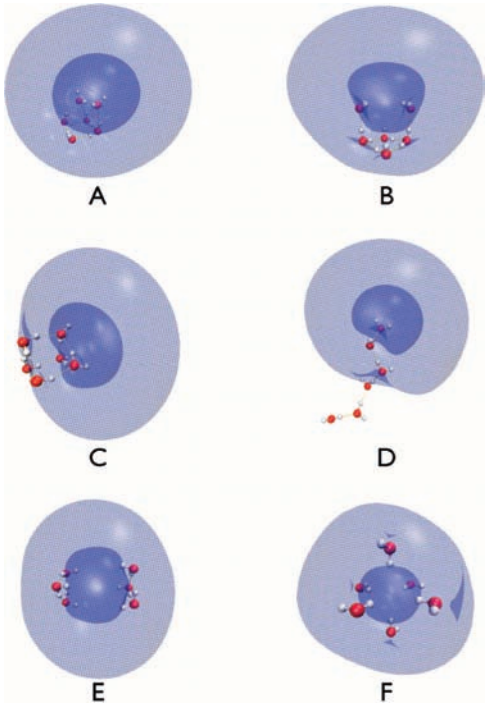

Figure 7. Six structures of $(H_2O)_6^-$ considered in this work. In each case, the charge density obtained from Drude model CI calculations is shown. The outer surface corresponds to the isosurface that encloses 90% of the charge, and the inner surface to the isosurface that encloses 70% of the charge.

discussed in section IIA, both correlation contributions beyond second order and the net correlation contributions are much larger in the Drude model than in the ab initio calculations. It is for this reason that a CI rather than a perturbative approach has been adopted in our applications of the Drude model. 6F is particularly interesting, in that, even though it does not bind the excess electron in the ES+rep and second-order Drude model treatments, the Drude model CI calculations give an EBE close to the ab initio CCSD(T) result.

Additional insight into the relative importance of various contributions to the EBEs is provided by Table 2, which reports for the six $(H_2O)_6^-$ isomers the kinetic energy, electrostatic, and repulsion contributions calculated using the ES+rep and Drude model CI approaches. (The PM3 results are close to those of the Drude CI calculations and, for that reason, have not been included in the table.) For the CI calculations, the correlation energy contributions to the EBE are also reported. For all six isomers, the kinetic energy contribution roughly doubles upon inclusion of the correlation contributions (with either the Drude or PM3 models), consistent with the excess electron being much more localized in the calculations including correlation effects.

Table 2 also includes values of the radius of gyration $R_g = (\langle r^2\rangle - \langle r\rangle^2)^{1/2}$ of the excess electron calculated at the ES+rep and Drude CI levels of theory. (The R_g values for the PM3 model are close to the corresponding Drude CI values.) The R_g values are typically about 3 Å smaller for the Drude CI and PM3 than for the ES+rep wave functions, again consistent with large contractions of the excess electron distributions upon inclusion of correlation effects. This is also seen from Figure 8 where the change distributions, at the 90% isodensity level, of the excess electron of 6A as described by the ES+rep and Drude CI approximations are plotted. (The R_g value for 6F, as described by the ES+rep model, is not meaningful as the excess electron is not bound in this approximation.) The origin of the contraction is obvious for the PM3 model as the inclusion of the polarization term makes the net potential more attractive at distances less than about 3 Å from the monomers. In the Drude CI calculations much of the contraction is due to coupling with single excitations of the excess electron (with none of the Drude oscillators excited). In a perturbative treatment such excitations do not enter the expression for the energy until fourth order, where they can become important due to small energy denominators. A sizable contraction of the electron density associated with the excess electron upon inclusion of correlation effects is also found in ab initio calculations of $(H_2O)_n^-$ clusters. Interestingly, for all six $(H_2O)_6^-$ isomers, the sum of the kinetic energy, electrostatic, and repulsive contributions to the Drude CI and PM3 energies

TABLE 2: Contributions to the Negatives of the EBEs (meV) and the Radius of Gyration R_g (Å) of the Excess Electron Distributions of the $(H_2O)_6^-$ Clusters

	6A		6B		6C		6D		6E		6F	
property[a]	KT	CI	KT	CI	KT	CI	KT	CI	KT	CI	KT	CI
EBE Contribution												
KE	345	654	411	805	252	580	255	514	426	846	12	1709
ES	−578	−918	−684	−1116	−418	−763	−433	−716	−621	−1109	−12	−2110
repul	63	256	93	329	43	265	49	183	134	347	4	654
sum	−171	−8	−180	17	−123	82	−129	−18	−60	84	4	253
correl		−443		−619		−465		−312		−649		−1088
total	−171	−451	−180	−592	−123	−383	−129	−330	−60	−565	4	−835
R_g	6.7	4.3	6.2	3.9	7.9	4.7	9.3	5.3	7.2	3.7		3.2

[a] KE, ES, repul., and correl. refer to the kinetic energy, electrostatic, repulsive, and correlation contributions, respectively, to the total EBEs, Sum refers to the sum of all contributions other than correlation.

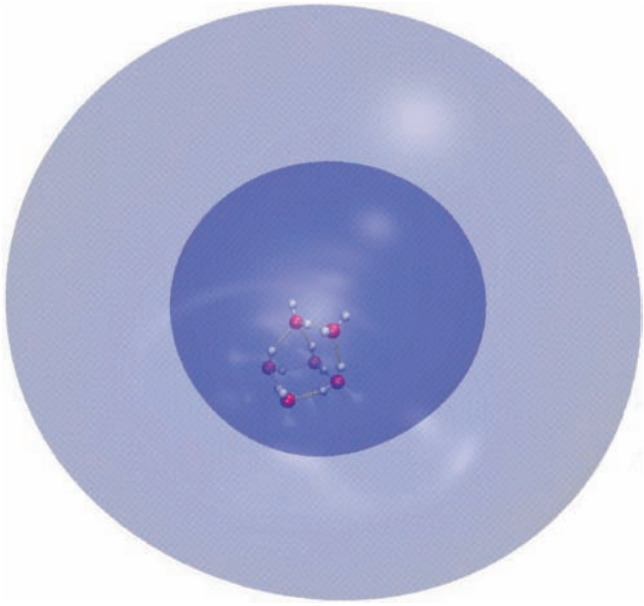

Figure 8. Contraction of the electron density of isomer 6A upon incorporation of correlation effects via CI calculations with the Drude model. Outer represents the electron density in the ES+rep model at the 90% isosurface level, and the inner represents the electron density in the Drude CI model, also at the 90% isosurface level.

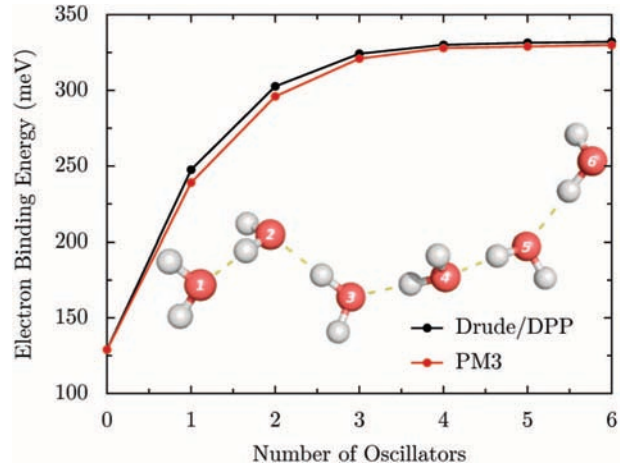

Figure 9. Electron binding of isomer 6D of $(H_2O)_6^-$ with sequential inclusion of Drude oscillators or polarizable sites. As seen from the figure, only for the three water molecules on the acceptor end of the chain are there sizable polarization (correlation) contributions to the EBE.

is very small, with the result being that the net EBEs are roughly equal to the correlation (polarization) contributions.

From Figure 4, it is seen that the polarization potential is negligible for $r \leq 4$ Å (as measured from the center-of-mass of a monomer. This suggests that for large clusters it will not be necessary to include the Drude oscillators or polarization potentials on water molecules far from the excess electron (allowing, of course, for the spatial extent of the electron distribution). To test this idea, we report in Figure 9 the EBE of the $(H_2O)_6^-$ chain (6D) with successive (starting from the end furthest from the excess electron) Drude oscillators or polarizable centers removed. From this figure, it is seen that the contribution of correlation (polarization) effects drops off rapidly along the chain with nearly the full contribution being recovered when Drude oscillators (polarization centers) are included on only the three waters on the acceptor end of the chain (i.e., the end of the chain to which the excess electron is bound). It is noteworthy that nearly identical correlation contributions from the different monomers are obtained in the Drude CI and PM3 model potential approaches. This result confirms that for large clusters and for simulations of e_{aq}^- it will be necessary to employ Drude oscillators (or polarizable sites) on only a relatively small subset of the water monomers, thereby greatly reducing the computational cost of the calculations. The challenge, of course, is to introduce a computationally fast procedure for estimating the charge distribution of the excess electron, which can be then used to decide on which water monomers to include Drude oscillators or polarizable sites. One potential strategy for accomplishing this is to first carry out PM3 model calculations using a small set of *s* Gaussian functions distributed on a 3D grid or small DVR basis set.

For the four $(H_2O)_6$ isomers with large dipole moments, the Drude model CI and PM3 models give EBEs that agree to within 4%. However, for 6E and 6F, with zero dipole moments and "cavity-bound" anion states, the PM3 values of the EBEs are, respectively, 9 and 17% larger than the Drude CI values, with the latter being in closer agreement with the ab initio CCSD(T) results. As will be seen below, the PM3 model consistently gives larger EBEs than the Drude model, with the difference generally being the greatest in the case of cavity-bound anions.

For the six $(H_2O)_6^-$ clusters the EBEs from the TB polarization model are in poorer agreement with the ab initio CCSD(T) results than are the EBEs from the Drude model CI or the PM3 polarization model calculations, with the average absolute difference between the TB and CCSD(T) EBEs being 30%. With the exception of 6E, the TB model gives smaller EBEs than do the Drude model or ab initio CCSD(T) calculations. Examination of the individual contributions to the EBEs in Table 1 provides an explanation of this behavior. For all six $(H_2O)_6^-$ isomers, the polarization contribution to the energy is appreciably smaller in magnitude in the TB model than in the Drude and PM3

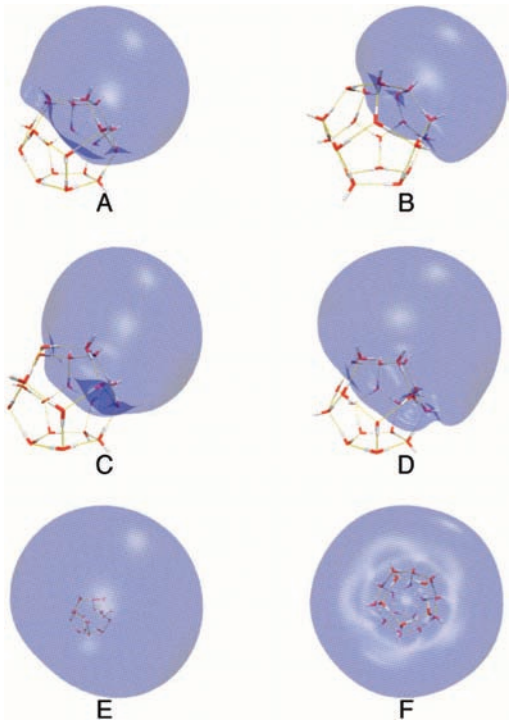

Figure 10. Isomers of $(H_2O)_{20}^-$ considered in this work. The isosurfaces enclosing 90% of the charge are shown.

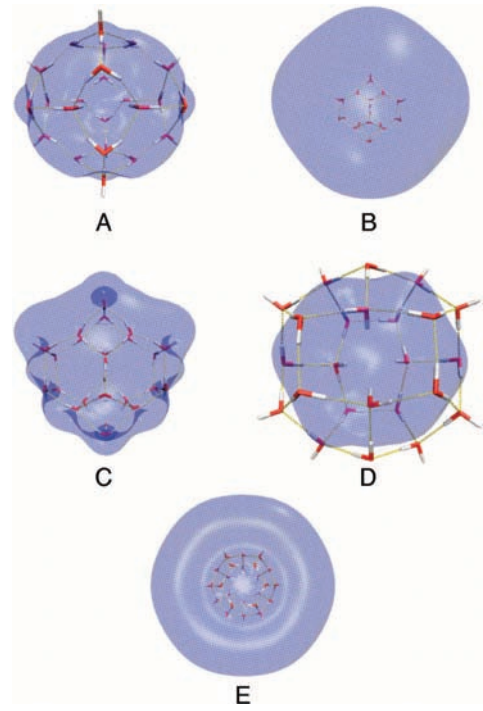

Figure 11. Isomers of $(H_2O)_{24}^-$ considered in this work. The isosurfaces enclosing 90% of the charge are shown.

models. (Here we have equated the correlation corrections in the Drude model with the polarization contributions in the polarization models.) With the exception of 6E, the electrostatic contributions to the total energy are roughly the same in the three models. On the other hand, for 6E, in which there are six OH groups, relatively close together, pointed toward the cavity center, the electrostatic contribution is about 1.6 times larger in the TB model than in the Drude or PM3 models, which more than compensates for the weak polarization in the TB approach. For the other five isomers, the enhanced electrostatic interactions in the TB model do not compensate for the underestimation of the polarization contribution.

C. Results for $(H_2O)_{20}^-$ and $(H_2O)_{24}^-$. The six $(H_2O)_{20}^-$ clusters considered in this work and depicted in Figure 10 all have dodecahedral structures that differ in the orientations of the OH groups, with dipole moments that range from 0 to 25 D. The five $(H_2O)_{24}^-$ clusters (Figure 11), on the other hand, all have zero dipole moments. These $(H_2O)_{20}^-$ and $(H_2O)_{24}^-$ structures are described in the papers of Herbert and Head-Gordon[19,20] and are expected to be appreciably less stable than the global potential energy minima. All six $(H_2O)_{20}^-$ clusters and two of the $(H_2O)_{24}^-$ clusters (24B and 24E) have surface-bound excess electron states. The other three $(H_2O)_{24}^-$ clusters have cavity-bound excess electron states.

For the four $(H_2O)_{20}$ clusters with large dipole moments, the EBE's obtained from the Drude model CI and PM3 approaches are in excellent agreement with each other and with the ab initio MP2 results of Herbert and Head-Gordon. However, for the $(H_2O)_{20}$ and $(H_2O)_{24}$ clusters with zero or near zero dipole moments, the situation is quite different. For these clusters, the Drude model CI and PM3 approaches give much larger EBEs than obtained from the MP2 calculations. The large differences between the model potential and ab initio MP2 EBEs for these species is largely a consequence of inadequacy of the Hartree−Fock reference wave functions rather than a deficiency of the Drude model or polarization model approaches. Indeed, for these clusters the Hartree−Fock calculations either fail to bind the excess electron or bind it only very weakly (with the exception of 24D).

Herbert and Head-Gordon devised an interesting strategy, referred to here as s-MP2(BHLYP), for dealing with the situation that the Hartree−Fock approximation fails to bind or only weakly binds the excess electron.[21] In this approach, the EBEs are calculated using the MP2 method, but with BHLYP[76,77] orbitals and orbital energies in place of the corresponding Hartree−Fock quantities, together with the application of a scaling factor. The success of the s-MP2(BHLYP) method stems from the fact that the BHLYP procedure binds the excess electron even in those cases where the Hartree−Fock method does not. For the seven $(H_2O)_{20}^-$ and $(H_2O)_{24}^-$ clusters with zero or near-zero dipole moments, the EBEs calculated with the s-MP2(BHLYP) procedure are in reasonable agreement with the Drude model CI results, with the average absolute difference, excluding 20F and 24B species, which bind the excess electron only weakly even in the Drude CI approach, being 21%. For the $(H_2O)_{20}$ clusters with large dipole moments, the MP2 and s-MP2(BHLYP) procedures give nearly the same EBEs, which, in turn, are close to the Drude model results.

Although the s-MP2 (BHLYP) method solves the major problem associated with MP2 calculations for $(H_2O)_n^-$ clusters for which the Hartree−Fock method does not provide a suitable zeroth-order wave function, it is likely that the Drude model CI approach provides more accurate estimates of the EBEs for these clusters. There is a need for high quality ab initio calculations of the EBEs for clusters such as 20E, 20F, and 24A−24E to determine whether this is indeed the case. Such calculations will be very challenging because they will require an approach such as EOM-CCSD that does not require the excess electron to be bound in the Hartree−Fock approximation, together with the use of large, flexible basis sets. For systems of the size of $(H_2O)_{24}^-$, such calculations would require a direct implementation of the EOM-CCSD algorithm.

For the $(H_2O)_{20}$ and $(H_2O)_{24}$ clusters with zero or near-zero dipole moment the PM3 approach gives larger (by up to 50%)

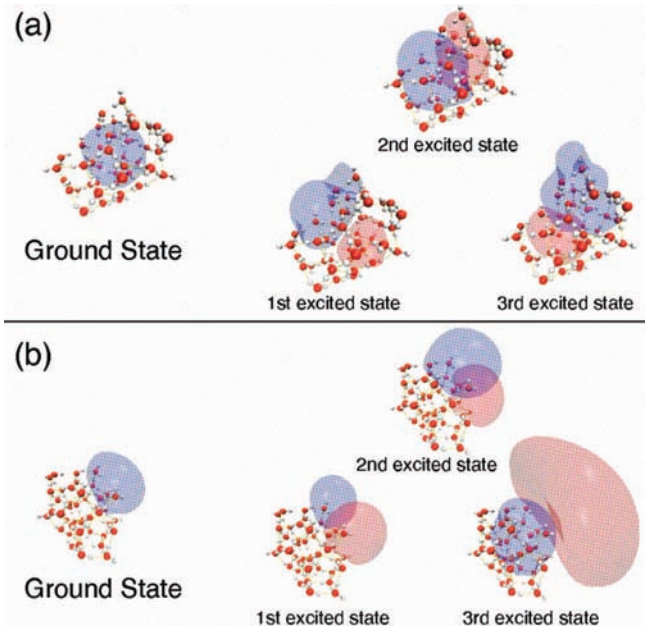

Figure 12. Natural orbitals of the ground and low-lying electronically excited states of the anions of 45A and 45B (a), and (b), respectively. The surfaces drawn correspond to 70% isodensities.

EBEs than obtained with the Drude model CI approach, whereas for the clusters with large dipole moments these two approaches give similar values for the EBEs. As noted above, for 6E and 6F, which also have zero dipole moments, the PM3 method overestimates the EBEs by about 11%. The reason for the greater disparity between the Drude model and PM3 values of the EBEs for these larger clusters is not clear. However, it should be recalled that the damping parameters in the two models were chosen so that the model potentials reproduce the CCSD(T) value of the EBE of $(H_2O)_2^-$, which is a dipole-bound anion, with an EBE of only about 40 meV and a much more extended charge distribution than for the cavity-bound anions of $(H_2O)_{20}$ and $(H_2O)_{24}$.

On the basis of the results for 6E and 6F, we anticipate that, in general, the Drude model provides more accurate estimates of the EBEs than does the PM3 polarization model. Again, calculations using a method such as EOM-CCSD will be required to establish this. We note also that the overall agreement between the EBEs calculated using the PM3 and the Drude models for the entire set of clusters considered can be improved by more strongly damping the polarization term in the PM3 model.

For all ten $(H_2O)_{20}^-$ and $(H_2O)_{24}^-$ clusters the TB model gives appreciably smaller EBEs than obtained from Drude model CI calculations. The ratio of the EBEs from the Drude model CI and TB methods ranges from 1.4 to 1.6 for the clusters with large dipole moments and from 1.6 to 4.0 for the clusters with zero or near zero dipole moments, excluding 24C, for which the ratio is 21. As discussed above for the $(H_2O)_6^-$ isomers, the weaker electron binding in the TB model is primarily a consequence of its weak polarization potential.

D. $(H_2O)_{45}^-$ Clusters. The two $(H_2O)_{45}^-$ clusters chosen for study are low-energy species identified in molecular dynamics simulations of Turi and Rossky.[32] As seen from Figure 12, the excess electron is localized in the interior of the cluster in 45A and is surface bound in 45B. For $(H_2O)_{45}^-$ there are no ab initio results with which to compare. Both $(H_2O)_{45}^-$ isomers bind the excess electron by about 700 meV in the ES+rep approximation. For 45A, the EBEs calculated from the Drude model CI, PM3, and TB calculations are 2508, 2861 and 2356 meV, respectively, whereas for 45B, the corresponding EBEs are 1350, 1480, and 986 meV. Thus, electron correlation effects contribute over 1 eV more to the EBE of 45A than to that of 45B, consistent with there being several more water monomers "close" to the excess electron in 45A than in 45B.

In the Drude CI calculations the radius of gyration of the excess electron is 2.2 and 3.5 Å for 45A and 45B, respectively. Interestingly, the radius of gyration calculated for the cavity-bound anion of 45A is close to the radius of e_{aq}^-. For both 45A and 45B, the EBE calculated using the PM3 model is only about 10% larger than that calculated using the Drude CI approach. In contrast, the TB approach gives smaller EBEs than does the Drude model CI method, with the differences being 6 and 29% for 45A and 45B, respectively. 45A, like 6E discussed above, has multiple OH groups pointing toward the excess electron which causes a large overestimation of the electrostatic contribution to the EBE in the TB model, which partially compensates for the underestimation of the polarization contribution in this approach.

E. Reliability of Model Potential Approaches for Predicting Relative Energies of $(H_2O)_n^-$ Isomers. Although the focus of this article has been on the use of model potential approaches for calculating EBEs of $(H_2O)_n^-$ clusters, equally important is the use of these approaches for predicting the relative stability of different isomers of these clusters. This requires that the model potential be able to accurately predict both the EBEs and the relative energies of the neutral clusters. Most model potential studies of $(H_2O)_n^-$ clusters have employed nonpolarizable SPC[73] or SPC/E[78] force fields, which are known to fare poorly in describing the energetics of neutral water clusters.[79] This can be seen from Table 3 which compares the relative energies of the neutral 6A−6F clusters, at the anion calculations. Results are presented at the ab initio CCSD(T)/aug-cc-pVTZ[80] level: and with the SPC and DPP force fields, which are used in the TB and Drude (and PM3) models, respectively. It is seen from this table that the DPP water model is more successful at reproducing the relative energies of the neutral clusters than is the SPC model, with the average absolute errors, determined by comparison with the CCSD(T) results, being 3.6 and 229 meV with the DPP and SPC models, respectively. In our earlier versions of the quantum Drude model we adopted the polarizable Dang−Chang model[81] for the water force field. Although the Dang−Chang model has proven successful for describing water in a range of environments, we have found that it does not do a good job at describing the relative energies of the neutral clusters at the geometries adopted in the anions. Indeed, this is what motivated us to develop the DPP model, which fares much better in this regard.

Table 3 also includes the relative energies of the anions of 6A−6F calculated using the various theoretical methods. As expected, the Drude/DPP approach gives relative energies close to the CCSD(T) results, whereas the TB/SPC method gives relative energies differing by as much as 621 meV from the CCSD(T) results. Excluding the artificial system 6F, the Drude/DPP calculations give the relative energies of the anionic species correct to 31 meV (0.7 kcal/mol). However, the Drude/DPP calculations predict the anion of 6F to be 1430 meV less stable than that of 6A, whereas the CCSD(T) calculations give an energy difference of 1518 meV.

F. Excited States. Experimentally, it has been found that for the $(H_2O)_n^-$, $n \leq 6$ ions, vertical excitation of the excess electron leads to direct photodetachment to the continuum, whereas for the $n \geq 15$ clusters, vertical excitation assesses bound (with

TABLE 3: Relative Energies (meV) of the Various Forms of $(H_2O)_6^-$ and of $(H_2O)_6$ at the Geometries of the Anions[a]

	6B		6C		6D		6E		6F	
	neutral	anion	neutral	anion	neutral	anion	neutral	anion	neutral	anion
DPP	290	172	−27	50	265	384	604	490	1814	1430
SPC	442	259	−48	7	109	252	908	605	2213	2139
MP2[b]	293	153	−102	22	273	343	557	467	1841	1497
CCSD(T)[b]	293	153	−112	19	293	383	549	469	1824	1518

[a] The energies of the neutral cluster are given relative to that of 6A, and those of the anions are given relative to that of the anion of 6A. [b] The ab initio results for 6A−6E are from ref 39.

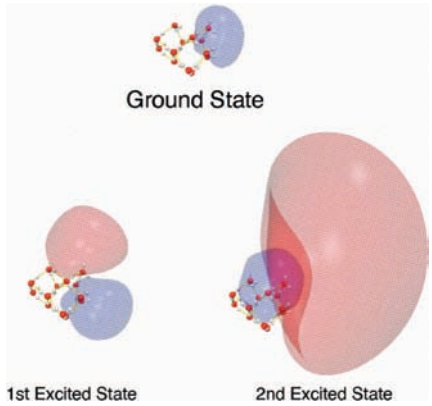

Figure 13. Natural orbitals of the ground and low-lying electronically excited states of an AA isomer of $(H_2O)_{13}^-$. The surfaces drawn correspond to 70% isodensities.

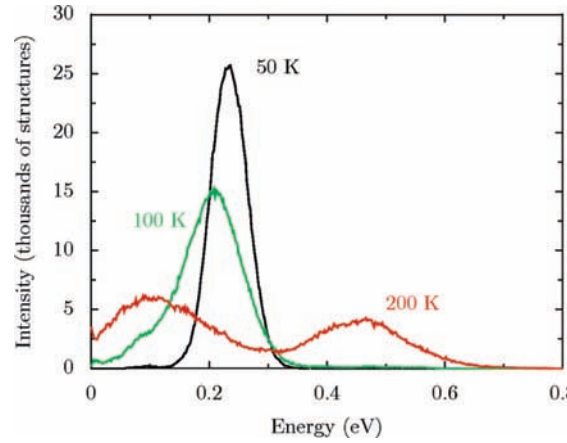

Figure 14. Electron-binding energy distributions of $(H_2O)_7^-$ from parallel tempering Monte Carlo simulations. Results are shown for T = 50, 100, and 200 K.

respect to electron detachment) excited states.[82] Both the Drude model CI and the polarization model approaches are able to describe these excited states of $(H_2O)_n^-$ clusters, although the lack of ab initio data on the excited states prevents us from assessing the accuracy of the model potential approaches for characterizing these species. However, given the fact that the excited-state wave functions are much more spatially extended than the ground-state wave functions, it is reasonable to expect that the Drude and PM3 model potential approaches perform even better for the excited states than for the ground states.

Although the geometrical structures of the observed $(H_2O)_n^-$, $n \geq 8$, ions are unknown, there is evidence that species with AA electron "binding sites" are important at least up to n = 21.[27] For this reason, in comparing the various model potential approaches for describing the excited states of $(H_2O)_n^-$, we include a low-energy isomer of $(H_2O)_{13}^-$ with an AA binding site (Figure 13). We also report excitation energies and natural orbitals for 45A and 45B, which are representative of surface- and interior-bound species in the large cluster regime. Table 4 reports the excitation energies of these three clusters calculated using the Drude model CI, PM3, and TB approaches. The natural orbitals for the ground and lowest energy bound excited states as described by the Drude CI approach for the three clusters are shown in Figures 12 and 13.

For all three clusters the natural orbital of the ground state is approximately s-like and the natural orbitals of the low-lying excited states are p-like. Thus the electronic transitions can be qualitatively described as s → p independent of whether the excess electron is cavity- or surface-bound. This conclusion was also reached by Turi and Rossky in their recent study of $(H_2O)_n^-$ clusters.[32]

For the three clusters considered, the Drude and PM3 models give similar excitation energies, whereas the excitation energies from the TB model differ by up to 20% from the corresponding Drude model CI results. For the $(H_2O)_{13}^-$ cluster, the calculated excitation energy (Drude model) to the lowest excited state is 938 meV in reasonable agreement with experiment for the n = 15 cluster, for which the peak in the absorption spectrum occurs near 850 meV.[27]

G. Use of Model Potentials in Finite Temperature Simulations. One of the major motivations for developing model potential approaches for describing $(H_2O)_n^-$ clusters is to enable Monte Carlo and molecular dynamics simulations to better understand the finite temperature behavior and dynamics of the clusters. To date we have used the Drude model to carry out parallel tempering Monte Carlo (PTMC)[83] simulations on clusters as large as $(H_2O)_{13}^-$.

Here we briefly consider an application of PTMC simulations together with the Drude model approach to $(H_2O)_7^-$. The details of the simulations have been reported in ref 74. The temperatures employed in the simulations ranged from 30 to 200 K.[74] Figure 14 reports the electron binding energy distributions for T = 50, 100, and 200 K. Interestingly, the T = 50 and 100 K distributions are characterized by a peak near 0.1 eV, and only at high (e.g., T = 200 K) temperatures is there sizable population of clusters with EBEs ∼0.4 eV. This is in contrast with experiment for which the dominant species have EBEs near 0.45 eV.[26] This suggests that the clusters observed experimentally, are not representative of an equilibrium distribution. One of the grand challenges in the study of $(H_2O)_n^-$ ions is to be able to simulate the formation of the $(H_2O)_n^-$ ions under experimental conditions Model potential approaches such as those described in this paper will be essential for such an undertaking.

At present, Monte Carlo or molecular dynamics simulations of $(H_2O)_n^-$ clusters using the Drude model are limited to clusters containing about 15 water molecules. Simulations on much larger clusters are feasible with the polarization model approach, as the CI step present in the Drude model approach is eliminated. The size clusters that can be simulated in both approaches can be greatly increased through use of integral screening and parallelization of the code.

TABLE 4: Ground- and Excited-State Energies (meV) for $(H_2O)_{13}^-$ and $(H_2O)_{45}^-$ As Described by the Drude Cl, PM3, and TB Models

	13			45A			45B		
	C1	PM3	TB	C1	PM3	TB	Cl	PM3	TB
ground	−1119	−1173	−807	−2508	−2861	−2606	−1395	−1480	−1103
first	−182	−229	−106	−554	−762	−272	−599	−643	−374
second	−52	−68	−29	−471	−730	−192	−491	−572	−338
third		−2		−450	−709	−94	−205	−322	−135

IV. Conclusions

It is known from ab initio electronic structure calculations that electron correlation effects play a major role in the binding of excess electrons to water clusters. Our group has shown that these correlation effects can be accurately modeled by use of quantum Drude oscillators in which the ten electrons on each water monomer are modeled by a 3-dimensional Drude oscillator. In the present study, we have used an adiabatic separation between the excess electron and the Drude oscillators to derive a family of polarization potential models for the excess electron. This derivation demonstrates that one-electron models with polarization potential terms are able to recover correlation interactions between the excess electron and the more tightly bound electrons of the monomers. Thus we have a hierarchy of methods, starting with ab initio approaches in which all electrons are treated explicitly, the intermediate Drude model in which the dynamical response of the 10 electrons of each water molecule is modeled by a Drude oscillator, giving a simplified many-body problem, and finally, the polarization model approaches with one-particle Schrodinger equations. In the ab initio and Drude model approaches, recovery of the correlation effects between the excess electron and the electrons of the water monomers requires the inclusion of double excitations, whereas this is accomplished via incorporation of the polarization potential in the polarization model approach. For most clusters considered, the polarization potential approach gives electron binding energies in close agreement with the Drude model results, although for clusters with cavity-bound excess electron states, the EBEs from the polarization potential approach tend to be somewhat larger that the Drude model results.

Ab initio Hartree−Fock calculations do not provide a proper zeroth-order wave function of several of the clusters with zero or near zero dipole moments. Both the Drude model, when used in conjunction with the CI method, and the polarization model approaches provide realistic descriptions of the anion states for these challenging systems.

It has also been demonstrated that correlation (polarization) contributions from water molecules more than ∼4 Å from regions where the excess electron has appreciable density are unimportant, although, to exploit this computationally it will first be necessary to obtain a rough estimate of the distribution of the excess electron (e.g., using preliminary calculations with smaller basis sets). Such strategies will enable accurate calculations of the anion states of $(H_2O)_n$ clusters containing hundreds of monomers.

We also showed that to accurately describe the relative energies of the various isomers of a $(H_2O)_n^-$ cluster, it is essential to employ both a realistic model for the electron−water interaction and an accurate model for the neutral water clusters. Our work indicates that many popular water models do not meet the latter requirement.

In spite of the success of the Drude and polarization potential models demonstrated in this article, it should be kept in mind that neither the Drude nor the PM3 polarization model, in their present implementations, is fully self-consistent, in that the interaction between the excess electron and a water monomer does not alter the interaction with the other monomers. The model Hamiltonians can be readily modified to allow for such many-body interactions, and we plan to explore this extension in future studies.

Although the focus of this article has been on excess electrons interacting with water clusters, it is immediately obvious that accurate Drude or polarization model approaches can be designed for excess electrons interacting with clusters of other polar molecules such as methanol or ammonia. In addition, one can combine the model potential approaches described here with ab initio methods for use in theoretical characterization of $X^-(H_2O)_n$ systems, where the excess electron in X^- occupies a valence orbital and the water molecules are incorporated via the Drude or PM3 models. The methods that we have developed for describing excess electrons interacting with water clusters may also suggest new strategies for treating long-range correlation effects in other problems. For example, it is intriguing to speculate on the use of a Drude oscillator approach for describing long-range correlation effects in molecular dimers. We note also that there are similarities between our Drude-model approach and Becke and Johnson's exchange-hole approach for treating intermolecular dispersion.[84]

Acknowledgment. This research was carried out with the support of a grant from the National Science Foundation. We thank L. Turi for the copy of his computer code with the Turi−Borgis model for excess electrons interacting with water.

References and Notes

(1) Garrett, B. C.; Dixon, D. A.; Camaioni, D. M.; Chipman, D. M.; Johnson, M. A.; Jonah, C. D.; Kimmel, G. A.; Miller, J. H.; Rescigno, T. N.; Rossky, P. J.; Xantheas, S. S.; Colson, S. D.; Laufer, A. H.; Ray, D.; Barbara, P. F.; Bartels, D. M.; Becker, K. H.; Bowen, K. H.; Bradforth, S. E.; Carmichael, I.; Coe, J. V.; Corrales, L. R.; Cowin, J. P.; Dupuis, M.; Eisenthal, K. B.; Franz, J. A.; Gutowski, M. S.; Jordan, K. D.; Kay, B. D.; LaVerne, J. A.; Lymar, S. V.; Madey, T. E.; McCurdy, C. W.; Meisel, D.; Mukamel, S.; Nilsson, A. R.; Orlando, T. M.; Petrik, N. G.; Pimblott, S. M.; Rustad, J. R.; Schenter, G. K.; Singer, S. J.; Tokmakoff, A.; Wang, L.-S.; Wettig, C.; Zwier, T. S. *Chem. Rev.* **2005**, *105*, 355.

(2) Martinez, S. E.; Huang, D.; Ponomarev, M.; Cramer, W. A.; Smith, J. L. *Protein Sci.* **1996**, *5*, 1081.

(3) Weyl, W. *Ann. Phys. Chem.* **1864**, *123*, 350.

(4) Hart, E. J.; Boag, J. W. *J. Am. Chem. Soc.* **1962**, *84*, 4090.

(5) Mizuno, M.; Yamaguchi, S.; Tahara, T. *J. Phys. Chem. A* **2005**, *109*, 5257.

(6) Silva, C.; Walhout, P. K.; Yokoyama, K.; Barbara, P. F. *Phys. Rev. Lett.* **1998**, *80*, 1086.

(7) Kambhampati, P.; Son, D. H.; Kee, T. W.; Barbara, P. F. *J. Phys. Chem. A* **2002**, *106*, 2374.

(8) Pshenichnikov, M. S.; Baltuska, A.; Wiersma, D. A. *Chem. Phys. Lett.* **2004**, *389*, 171.

(9) Paik, D. H.; Lee, I.-R.; Yang, D.-S.; Baskin, J. S.; Zewail, A. H. *Science* **2004**, *306*, 672.

(10) Turi, L.; Borgis, D. *J. Chem. Phys.* **2002**, *117*, 6186.

(11) Schnitker, J.; Rossky, P. J. *J. Chem. Phys.* **1987**, *86*, 3471.

(12) Rosenthal, S. J.; Schwartz, B. J.; Rossky, P. J. *Chem. Phys. Lett.* **1994**, *229*, 443.

(13) Borgis, D.; Rossky, P. J.; Turi, L. *J. Chem. Phys.* **2006**, *125*, 064501.

(14) Feng, D.-F.; Kevan, L. *Chem. Rev.* **1980**, *80*, 1.

(15) Coe, J. V.; Lee, G. H.; Eaton, J. G.; Arnold, S. T.; Sarkas, H. W.; Bowen, K. H.; Ludewigt, C.; Haberland, H.; Worsnop, D. R. *J. Chem. Phys.* **1990**, *92*, 3980.
(16) Shkrob, I. A. *J. Phys. Chem. A* **2007**, *111*, 5223.
(17) Sobolewski, A. L.; Domcke, W. *Phys. Chem. Chem. Phys.* **2002**, *4*, 4.
(18) Lee, H. M.; Suh, S. B.; Kim, K. S. *J. Chem. Phys.* **2003**, *118*, 9981.
(19) Gutowski, M.; Skurski, P. *Recent Res. Dev. Phys. Chem.* **1999**, *3*, 245.
(20) Herbert, J. M.; Head-Gordon, M. *J. Phys. Chem. A* **2005**, *109*, 5217.
(21) Herbert, J. M.; Head-Gordon, M. *Phys. Chem. Chem. Phys.* **2006**, *8*, 68.
(22) Williams, C. F.; Herbert, J. M. *J. Phys. Chem. A* **2008**, *112*, 6171.
(23) Hammer, N. I.; Roscioli, J. R.; Johnson, M. A.; Myshakin, E. M.; Jordan, K. D. *J. Phys. Chem. A* **2005**, *109*, 11526.
(24) Shin, J.-W.; Hammer, N. I.; Headrick, J. M.; Johnson, M. A. *Chem. Phys. Lett.* **2004**, *399*, 349.
(25) Hammer, N. I.; Roscioli, J. R.; Johnson, M. A. *J. Phys. Chem. A* **2005**, *109*, 7896.
(26) Roscioli, J. R.; Hammer, N. I.; Johnson, M. A.; Diri, K.; Jordan, K. D. *J. Chem. Phys.* **2008**, *128*, 104314.
(27) Hammer, N. I.; Roscioli, J. R.; Bopp, J. C.; Headrick, J. M.; Johnson, M. A. *J. Chem. Phys.* **2005**, *123*, 244311.
(28) Roscioli, J. R.; Johnson, M. A. *J. Chem. Phys.* **2007**, *126*, 024307.
(29) Verlet, J. R. R.; Bragg, A. E.; Kammrath, A.; Cheshnovsky, O.; Neumark, D. M. *Science* **2005**, *307*, 93.
(30) Bragg, A. E.; Verlet, J. R. R.; Kammrath, A.; Cheshnovsky, O.; Neumark, D. M. *J. Am. Chem. Soc.* **2005**, *127*, 15283.
(31) Asmis, K. R.; Santambrogio, G.; Zhou, J.; Garand, E.; Headrick, J.; Goebbert, D.; Johnson, M. A.; Neumark, D. M. *J. Chem. Phys.* **2007**, *126*, 191105.
(32) Turi, L.; Sheu, W.-S.; Rossky, P. J. *Science* **2005**, *309*, 914.
(33) Turi, L.; Madarasz, A.; Rossky, P. J. *J. Chem. Phys.* **2006**, *125*, 014308.
(34) Haberland, H.; Schindler, H. G.; Worsnop, D. R. *Ber. Bunsen-Ges. Phys. Chem.* **1984**, *88*, 270.
(35) Weber, J. M.; Leber, E.; Ruf, M.-W.; Hotop, H. *Euro. Phys. J. D - Atom. Mol. Opt. Plasma Phys.* **1999**, *7*, 587.
(36) Gutowski, M.; Skurski, P.; Jordan, K. D.; Simons, J. *Int. J. Quantum Chem.* **1997**, *64*, 183.
(37) Gutowski, M.; Skurski, P.; Boldyrev, A. I.; Simons, J.; Jordan, K. D. *Phys. Rev. A* **1996**, *54*, 1906.
(38) Pople, J. A.; Head-Gordon, M.; Raghavachari, K. *J. Chem. Phys.* **1987**, *87*, 5968.
(39) Gutowski, M. Unpublished results.
(40) Koch, W.; Holthausen, M. C. *A Chemist's Guide to Density Functional Theory*, 2nd ed.; Wiley-VCH: New York, 2001.
(41) Cohen, A. J.; Mori-Sànchez, P.; Yang, W. *J. Chem. Phys.* **2007**, *127*, 034101.
(42) Barnett, R. N.; Landman, U.; Cleveland, C. L.; Jortner, J. *J. Chem. Phys.* **1988**, *88*, 4429.
(43) Nicolas, C. e. d.; Boutin, A.; Levy, B.; Borgis, D. *J. Chem. Phys.* **2003**, *118*, 9689.
(44) Wallqvist, A.; Martyna, G.; Berne, B. J. *J. Phys. Chem.* **1988**, *92*, 1721.
(45) Benjamin, I.; Evans, D.; Nitzan, A. *J. Chem. Phys.* **1997**, *106*, 6647.
(46) Rossky, P. J.
(47) Turi, L.; Gaigeot, M.-P.; Levy, N.; Borgis, D. *J. Chem. Phys.* **2001**, *114*, 7805.
(48) Wang, F.; Jordan, K. D. *J. Chem. Phys.* **2001**, *114*, 10717.
(49) Wang, F.; Jordan, K. D. *J. Chem. Phys.* **2002**, *116*, 6973.
(50) Sommerfeld, T.; Jordan, K. D. *J. Phys. Chem. A* **2005**, *109*, 11531.
(51) Sommerfeld, T.; Gardner, S. D.; DeFusco, A.; Jordan, K. D. *J. Chem. Phys.* **2006**, *125*, 174301.
(52) Sommerfeld, T.; Jordan, K. D. *J. Am. Chem. Soc.* **2006**, *128*, 5828.
(53) Jordan, K. D.; Wang, F. *Annu. Rev. Phys. Chem.* **2003**, *54*, 367.
(54) Rigby, M.; Smith, E. B.; Wakeham, W. A.; Maitland, G. C. *The Forces Between Molecules*; Oxford Science Publications: Oxford U.K., 1986.
(55) Jordan, K. D. *Acc. Chem. Res.* **1979**, *12*, 36.
(56) Simons, J.; Jordan, K. D. *Chem. Rev.* **1987**, *87*, 535.
(57) Wallis, R. F.; Herman, R.; Milnes, H. W. *J. Mol. Spectrosc.* **1960**, *4*, 51.
(58) Crawford, O. H. *Mol. Phys.* **1971**, *20*, 585.
(59) Landau, L. D. *Quantum Mechanics*; 2nd ed.; Pergamon Press: Oxford U.K., 1959; pp 118.
(60) Crawford, O. H.; Koch, B. J. D. *J. Chem. Phys.* **1974**, *60*, 4512.
(61) Garrett, W. R. *J. Chem. Phys.* **1982**, *77*, 3666.
(62) Born, M.; Oppenheimer, R. *Ann. Phys. (Leipzig)* **1927**, *84*, 457.
(63) Koopmans, T. *Physica* **1934**, *1*, 104.
(64) Stanton, J. F.; Bartlett, R. J. *J. Chem. Phys.* **1993**, *98*, 7029.
(65) Skurski, P.; Gutowski, M.; Simons, J. *Int. J. Quantum Chem.* **2000**, *80*, 1024.
(66) Frisch, M.; J.; Trucks, G. W.; Schlegel, H. B.; Scuseria, G. E.; Robb, M. A.; Cheeseman, J. R.; Montgomery, J. A., Jr.; Vreven, T.; Kudin, K. N.; Burant, J. C.; Millam, J. M.; Iyengar, S. S.; Tomasi, J.; Barone, V.; Mennucci, B.; Cossi, M.; Scalmani, G.; Rega, N.; Petersson, G. A.; Nakatsuji, H.; Hada, M.; Ehara, M.; Toyota, K.; Fukuda, R.; Hasegawa, J.; Ishida, M.; Nakajima, T.; Honda, Y.; Kitao, O.; Nakai, H.; Klene, M.; Li, X.; Knox, J. E.; Hratchian, H. P.; Cross, J. B.; Adamo, C.; Jaramillo, J.; Gomperts, R.; Stratmann, R. E.; Yazyev, O.; Austin, A. J.; Cammi, R.; Pomelli, C.; Ochterski, J. W.; Ayala, P. Y.; Morokuma, K.; Voth, G. A.; Salvador, P.; Dannenberg, J. J.; Zakrzewski, V. G.; Dapprich, S.; Daniels, A. D.; Strain, M. C.; Farkas, O.; Malick, D. K.; Rabuck, A. D.; Raghavachari, K.; Foresman, J. B.; Ortiz, J. V.; Cui, Q.; Baboul, A. G.; Clifford, S.; Cioslowski, J.; Stefanov, B. B.; Liu, G.; Liashenko, A.; Piskorz, P.; Komaromi, I.; Martin, R. L.; Fox, D. J.; Keith, T.; Al-Laham, M. A.; Peng, C. Y.; Nanayakkara, A.; Challacombe, M.; Gill, P. M. W.; Johnson, B.; Chen, W.; Wong, M. W.; Gonzalez, C.; Pople, J. A. *Gaussian 03*, revision D.01; Gaussian: Wallingford, CT, 2004.
(67) DeFusco, A.; Schofield, D. P.; Jordan, K. D. *Mol. Phys.* **2007**, *105*, 2681.
(68) Murphy, W. F. *J. Chem. Phys.* **1977**, *67*, 5877.
(69) Petrov, I. D.; Sukhorukov, V. L.; Hotop, H. *J. Phys. B: Atom. Mol. Opt. Phys.* **1999**, *32*, n/a.
(70) Nicklass, A.; Stoll, H. *Mol. Phys.* **1995**, *86*, 317.
(71) Morrison, M. A.; Saha, B. C.; Gibson, T. L. *Phys. Rev. A* **1987**, *36*, 3682.
(72) Light, J. C.; Carrington, T. *Adv. Chem. Phys.* **2000**, *114*, 263.
(73) Berendsen, H. J. C.; Postma, J. P. M.; van Gunsteren, W. F.; Hermans, J. *Intermolecular Forces*; Reidel: Dordrecht, The Netherlands, 1981.
(74) DeFusco, A.; Sommerfeld, T.; Jordan, K. D. *Chem. Phys. Lett.* **2008**, *455*, 135.
(75) Sommerfeld, T.; Jordan, K. D., unpublished results.
(76) Becke, A. D. *J. Chem. Phys.* **1993**, *98*, 1372.
(77) Lee, C.; Yang, W.; Parr, R. G. *Phys. Rev. B.* **1988**, *37*, 785.
(78) Berendsen, H. J. C.; Grigera, J. R.; Straatsma, T. P. *J. Phys. Chem.* **1987**, *91*, 6269.
(79) Pedulla, J. M.; Kim, K.; Jordan, K. D. *Chem. Phys. Lett.* **1988**, *291*, 78.
(80) Dunning, T. H., Jr. *J. Chem. Phys.* **1989**, *90*, 1007.
(81) Dang, L. X.; Chang, T. M. *J. Chem. Phys.* **1997**, *106*, 8149.
(82) Ayotte, P.; Johnson, M. A. *J. Chem. Phys.* **1997**, *106*, 811.
(83) Earl, D. J.; Deem, M. W. *Phys. Chem. Chem. Phys.* **2005**, *7*, 3910.
(84) Becke, A. D.; Johnson, E. R. *Chem. Phys. Lett.* **2006**, *432*, 600.

JP806077H